Supplementary material

Appendix

A1. Determination of calcite dissolution rate k_1 , k_2

The multiple parameter model is built and equation (17) could be used to quantity the fracture aperture evolution in shale fractures. However, three critical parameters k_1 , k_2 and R_c should be decided before forecast permeability evolution.

k_1 is the dissolution rate of mineral on contacting asperities where pressure solution happens while k_2 is dissolution of mineral on free-face area where free-face dissolution occurs. However, in our experiment, one limitation of our research is impossibility of measuring the fluid acidity on the contacting asperities.

As for k_1 value, studies show that during core flooding experiments, the fluid is considered to be stagnant at the contacting asperities due to the water film effect and hydronium irons are consumed for calcite dissolution by stagnant water film which will result to a fluid acidity on contacting asperities decreases very quickly [1]. Researches show that when the fluid pH value larger than 6.0, the change of calcite rate dissolution is not significant[2,3]. Considering high reactivity of calcite, it is reasonable to assume the k_1 equals to calcite dissolution rate under neutral condition and the k_1 value is set as 7.39×10^{-7} mol/m^{2}s during calculation [1].

As for k_2 value, which means mineral dissolution rate in free-face area. Studies showed that dissolution rate of calcite (7.39×10^{-7} mol/m^{2}s) is much higher than quartz (2.51×10^{-9} mol/m^{2}s) under neutral condition (pH=7). In addition, calcite mineral has a larger dissolution rate when the fluid acidity is higher and quartz dissolution rate is almost not affected by fluid acidity. Compared with mineral compositions in shale, calcite mineral plays a dominant role in fracture aperture evolution through pressure solution and free-face dissolution process. Hence, k_2 value in equation (17) could be replaced by the dissolution rate of calcite which neglects the quartz mineral due to its low dissolution rate even though its content is pretty large in shale.

The calcite dissolution rate is controlled by PWP equation [2] and its value has been obtained under different pH conditions [3]. For our experimental conditions, the values are listed in **Table A1**.

Table A1 Calcite dissolution used in multiple parameter model

Fluid pH	k_1 **(mol/m^{2}s)**	k_2 **(mol/m^{2}s)**
4.0	7.39×10^{-7}	9.23×10^{-5}
5.0	7.39×10^{-7}	9.55×10^{-6}
6.0	7.39×10^{-7}	1.12×10^{-6}
7.0	7.39×10^{-7}	7.39×10^{-7}

A2. Determination of relationship between contact area ratio (R_c) and confining stress

The contact-area ratio (R_c) is another crucial parameter in multiple parameter model to forecast fracture aperture evolution. Research showed that contact-area ratio is only controlled by confining stress[4]. As mentioned before, one limitation of our research is impossibility to measure contact-area ratio directly. Here, we use effective hydraulic aperture as a bridge: firstly, the relationship between contact-area ratio and effective hydraulic aperture is built by profilometry method; then, the relationship between fracture aperture and confining stress is constrained by experiment. Combing the profilometry results and experimental data, the relationship between fracture effective hydraulic aperture and confining stress is fitted for different shale.

Longmaxi shale is chosen as an example to describe the fitting process.

The relationship between fracture aperture and contact-area ratio could be obtained by profilometry method [5,6] and tomography in a fracture surface could be described by Gaussian distribution [4]:

$$f(h) = \frac{1}{\sqrt{2\pi\sigma_h{}^2}} \exp(-\frac{h - \langle h^2 \rangle}{2\sigma_h{}^2}) \qquad \text{(A1)}$$

In this equation, h is the altitude of fracture surface, σ_h is the root-mean square and $\langle h \rangle$ is statistical average of fracture surface.

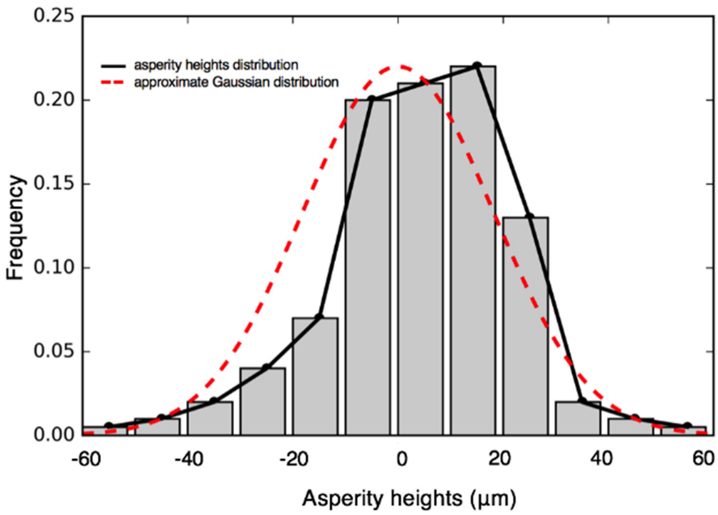

Figure A1. The height distribution in Longmaxi shale surface

The height distribution of Longmaix shale is shown in **Figure A1** which is accordance with Gaussian distribution. Firstly, the data is de-skewed and through maintaining the mean planes of fractures parallel, aperture distribution could be determined from point-by-point subtraction of two digitized surface and the arithmetic average aperture is calculated. The contact-area ratio is the number of overlapped datum points between two fracture surfaces. Then, by changing the relative position of two fracture surface, the accordingly relationship between contact-area ratio and fracture aperture is shown in **Figure A2**.

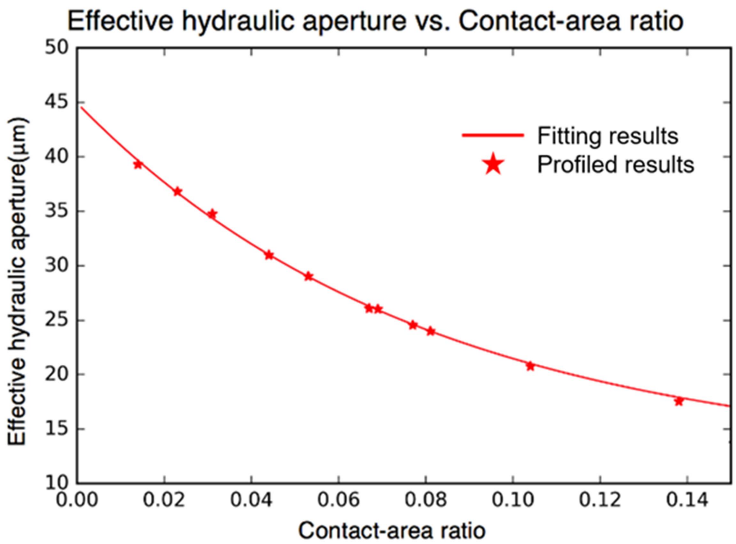

Figure A2. The relation between effective hydraulic aperture and contact area ratio

Then, based on regression curve, the relationship between effective hydraulic aperture and contact area ratio is given by:

$$e_h = a_1 + a_2 \exp(-R_c / a_3) \quad \text{(A2)}$$

where e_h is fracture aperture, R_c is contact-area ratio; a_1, a_2 and a_3 are constant.

It should be noted that only a_3 decide the curve shape and a_1 means the initial aperture of fracture surface and a_2 is the initial fracture aperture minus minimum fracture aperture.

After data fitting, the relationship between fracture aperture and contact-area ratio could be expressed as:

$$e_h = 12.05 + 32.89 \times \exp(-R_c / 0.08) \quad \text{(A3)}$$

Next, we further constrain the relationship between effective hydraulic aperture and confining stress by experiment. By adjusting the confining stress, the fracture aperture could be estimated by flow rate and results are shown in **Figure A3**.

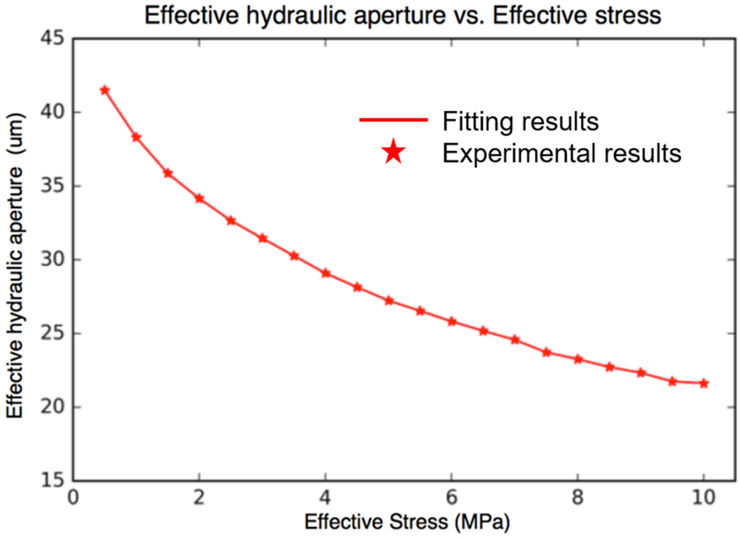

Figure A3. The relation between effective hydraulic aperture and effective stress

Confining stress will directly close the fracture aperture, which could be describe by the model [7]:

$$\Delta e_h = \frac{e_{h(0)} - e_{h(\mathrm{r})}}{1 + \dfrac{K_{nf} \cdot (e_{h(0)} - e_{h(\mathrm{r})})}{\sigma_n}} \quad \text{(A4)}$$

where K_{nf} is the fracture normal stiffness to describe the fracture's ability to resist normal stress $e_{h(0)}$ is the initial fracture aperture and $e_{h(\mathrm{r})}$ is the residential fracture aperture σ_n is the confining stress.

After data fitting, the relationship between fracture aperture and confining stress for Longmaxi shale could be expressed as:

$$e_h = 44.94 - \frac{32.89 \cdot \sigma_{conf}}{\sigma_{conf} + 4.1343} \quad \text{(A5)}$$

Based on above analysis, the relationship between fracture aperture and contact-area ratio could be expressed as:

$$e_h = 12.05 + 32.89 \times \exp(-R_c / 0.08) \quad \text{(A6)}$$

The relationship between contact-area ratio and confining stress could be get as and contact-area ratio for Longmaxi shale could be expressed as equation **A7** and plot in **Figure A4**:

$$R_c = -0.08\ln\left(1 - \frac{1}{1 + \frac{4.1352}{\sigma_{conf}}}\right) \tag{A7}$$

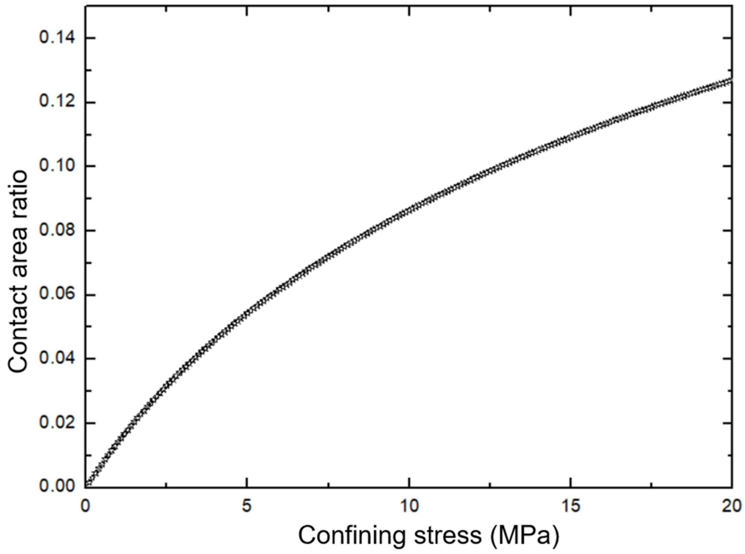

Figure A4. The fitting relation between contact-area ratio and effective stress

For our experiment conditions, the R_c values we used is showed in **Table A2**.

Table. A2 The contact area ratio used in model

Confining stress (MPa)	R_c (Longmaxi shale)	R_c (Green River shale)
3	4.4%	-
5	6.3%	-
10	9.8%	9.1%

A3. The simplification process from Eq.（17）to Eq. (18)

Except for phyllosilicate, the main mineral in Marcellus shale is quartz, who accounts for 36.1% of total weight percentage(As shown in Table 1). As mentioned in equation (7), the critical stress for quartz pressure solution is calculated as:

$$\sigma_c = \frac{E_m(1-\frac{T}{T_m})}{4V_m} \quad (7)$$

where E_m and T_m are heat and temperature of fusion. At room temperature (25℃), the calculated critical stress is 8520 MPa for quartz. Hence, in our experiments, the maximum confining stress is 10 MPa and the stress on contacting asperities is 227.27 MPa (confining stress/contact-area ratio). Hence, the quartz pressure solution can be neglected in our tests.

In addition, the free-face dissolution is largely controlled by fluid acidity. The dissolution rate of quartz under various fluid acidity is summarized in following **Table A3**.

The fracture aperture increasing rate contributed by quartz free-face dissolution is calculated based on following equation:

$$\frac{de_h}{dt} = 2(1-R_c)\cdot V_m \cdot k_2 \quad (A8)$$

Table A3. Comparison between fracture aperture changing rate caused by quartz free-face dissolution and clay swelling

Fluid pH	Quartz dissolution rate (mol/m^{2}s)	*Rc*	*Vm* (mol^{-1})	de_h/dt caused by quartz free-face dissolution (μm/min)	de_h/dt caused by clay swelling (μm/min)
4.0	1.27×10^{-12}	0.10	2.27×10^{-5}	3.08×10^{-9}	-2.33
5.0	1.99×10^{-12}	0.10	2.27×10^{-5}	4.89×10^{-9}	-2.54
6.0	1.00×10^{-11}	0.10	2.27×10^{-5}	2.45×10^{-8}	-3.00
7.0	1.26×10^{-11}	0.10	2.27×10^{-5}	3.09×10^{-8}	-3.15

Based on **Table A3**, the fracture aperture increasing rate caused by quartz free-face dissolution is ~ 10^{-9} μm/min, while decreasing rate caused by clay mineral swelling is several microns per minute. Hence, the quartz free-face dissolution is also neglected in analyzing Marcellus shale fracture aperture evolution.

Reference

[1] Ishibashi T, McGuire TP, Watanabe N, Tsuchiya N, Elsworth D. Permeability evolution in carbonate fractures: Competing roles of confining stress and fluid pH. Water Resour Res 2013;49:2828–42. doi:10.1002/wrcr.20253.

[2] Plummer LN, Wigley TML, Parkhurst DL. The kinetics of calcite dissolution in CO_2-water systems at 5℃ to 60℃ and 0.0 to 1.0 atm CO_2. Am J Sci 1978;278:179–216. doi:10.2475/ajs.278.2.179.

[3] Chou L, Garrels RM, Wollast R. Comparative study of the kinetics and mechanisms of dissolution of carbonate minerals. Chem Geol 1989;78:269–82. doi:10.1016/0009-2541(89)90063-6.

[4] Yasuhara H. Evolution of permeability in a natural fracture: Significant role of pressure solution. J Geophys Res 2004;109:B03204. doi:10.1029/2003JB002663.

[5] Stesky RM, S. S. Hannan. Growth of contact area between rough surfaces under normal stress. Geophys Res Lett 1987;14:550–3.

[6] Re F, Scavia C. Determination of contact areas in rock joints by X-ray computer tomography. Int J Rock Mech Min Sci 1999;36:883–90. doi:10.1016/S0148-9062(99)00056-X.

[7] Bandis SC, Lumsden AC, Barton NR. Fundamentals of rock joint deformation. Int J Rock Mech Min Sci 1983;20:249–68. doi:10.1016/0148-9062(83)90595-8.